Ossi Kimmelma, Ilkka Tittonen, and Scott C. Buchter. 2008. Short pulse, diode pumped, passively Q-switched Nd:YAG laser at 946 nm quadrupled for UV production. Journal of the European Optical Society - Rapid Publications, volume 3, 08008, 5 pages.

Short pulse, diode pumped, passively Q-switched Nd:YAG laser at 946 nm quadrupled for UV production

Ossi Kimmelma
Ossi.Kimmelma@tkk.fi
Department of Micro and Nanosciences and Center for New Materials, Micronova, Helsinki University of Technology, FI-02150 Espoo, Finland

Ilkka Tittonen
Department of Micro and Nanosciences and Center for New Materials, Micronova, Helsinki University of Technology, FI-02150 Espoo, Finland

Scott C. Buchter
Arctic Photonics, Jorvas Hitech Center, Hirsalantie 11, FI-02420 Jorvas, Finland

We report on a compact UV-laser with a short pulse length of 1.9 ns at 236 nm. A passively Q-switched quasi-three-level Nd:YAG laser at 946 nm acts as the pump source. UV pulses are produced by two consecutive single-pass frequency doubling events, the first one from IR to blue with a BIBO crystal and the second one from blue to deep-UV with a β-BBO crystal. Conversion efficiency from 946 nm to 473 nm is 28% and from blue to UV 7%. Average power for UV is 7.6 mW with a energy and peak power of 230 nJ, and 120 W respectively. [DOI: 10.2971/jeos.2008.08008]

Keywords: Solid state lasers, passively Q-switched lasers, quasi-three-level lasers, UV-lasers, nonlinear optics

1 INTRODUCTION

Compact laser sources delivering short pulses with high energy are appreciated in various applications especially in the UV wavelength range. Here we propose laser producing short pulses in the blue and deep-UV spectral ranges. This is realized by frequency doubling the light of a laser operating on the quasi-three-level transition of the Nd : $Y_3Al_5O_{12}$ (Nd:YAG) crystal at 946 nm. Focusing the high peak power laser with good beam quality into a nonlinear crystal is sufficient for an efficient frequency conversion. This is more straightforward than using a conversion setup with an optical resonator. The single-pass method is enabled by high peak power pulses.

Some commercial laser sources operating in a pulsed mode are already available for wavelengths below 250 nm. HeAg and NeCu UV lasers offer quasi-CW operation with average powers up to 0.4 mW and peak powers up to 250 mW [1]. Other ways to realize deep UV lasers include frequency doubling of Argon-ion based lasers and frequency quadrupling of mode locked solid state lasers. The former are however bulky and power consuming while the latter are essentially more complex than the particular laser design described in this paper. Most materials show high absorbance for wavelengths below 250 nm and thus this kind of laser sources can be used in materials processing. This short wavelength is also useful in semiconductor inspection and lithography. In addition, applications like fluorescence lifetime measurement require short pulses. The pulse lengths of interest are typically in the range of a few nanoseconds. The exciting pulse leading to fluorescence is preferred to be even shorter. Short pulses are also useful in applications that require high temporary peak power even though there is a risk to damage the material with high energy pulses. A quadrupled 946 nm laser gives output at 236 nm. Such a deep-UV light source has special use in resonant Raman spectroscopy, especially in studies of proteins [2] where the fluorescence band does not overlap with the Raman band giving a fluorescence-free signal. Quadrupling 946 nm light using nonlinear crystals is usually relatively inefficient because of the low effective nonlinearity in the UV-spectral range at room temperature. This conversion is further reduced by the Poynting-vector walk-off.

High peak power of the created pulses is essential for the operation of the laser design described here. Previously reported highest peak power obtained using a passively Q-switched Nd:YAG laser at 946 nm is 3.7 kW with the pulse width of 4.3 ns and unpolarised output [3]. Johansson *et al.* reported a passively Q-switched, frequency quadrupled laser with the fundamental peak power of 2.9 kW using a composite laser crystal [4]. Gerstenberger *et al.* [5] and Johansson *et al.* have reported an efficient quadrupling of 946 nm light in to 236 nm. In both these works a PPKTP crystal was used in a conversion from 946 nm to 473 nm. Gerstenberger used an actively Q-switched laser as a pump source and achieved a blue to UV conversion efficiency of 23% with a highly hygroscopic crystal of cesium lithium borate (CLBO) operated at -15°C. Johansson used a β-barium borate ($\beta-$BBO) crystal and achieved a 4.8 % conversion from blue to UV with the fundamental wavelength pulse length of 16 ns. In this work we concentrate on a laser design for achieving a short pulse length and high peak power with the fundamental pulse length of 3.5 ns. The frequency doubling from IR to blue is realized with a birefringently phase-matched BiB_3O_6 (BIBO) crystal followed by a conversion from blue to UV in a $\beta-$BBO crystal. Passively Q-switched lasers using birefringently phasematched nonlinear crystals at 236 nm have not been available. To our knowledge, at this short wavelengths a combination of short pulses and

Received November 14, 2007; published February 6, 2008 ISSN 1990-2573

high peak power has not been reported earlier using a passively Q-switched laser.

2 LASER DESIGN

The cavity photon lifetime of the laser is reduced for short pulse formation. This is primarily done by minimizing the optical length of the cavity. Short cavity results to small laser mode size. The mode affects the intensity inside the laser cavity as well as on the laser pulse energy. The laser cavity is made shorter by minimizing the free space in the laser resonator, and by choosing a relatively short laser crystal of 1.5 mm. This short cavity design excludes the possibility of using a composite laser crystal with undoped end caps in order to reduce the end bulging and for enhancing the thermal conduction used in many high average power lasers. There is also a trade off between the pump power absorption and the laser crystal length. With the used quasi-three-level laser transition, which has some absorption at the laser wavelength, our desire was to bleach the crystal with the pump power creating an effective optical aperture in the crystal and reduce the losses at the lasing wavelength. A limitation to this laser design is set by the damage threshold of the materials which is typically in the range of 500 MW/cm^2 for commercial coatings; a pulse with short length and high energy has high peak power which together with the small laser mode area leads to large intensity.

YAG crystal has a cubic crystal structure. In order to obtain a polarised output from the laser that is necessary in the second harmonic conversion, anisotropic response needs to be generated in the crystal. A pumping diode laser with stacked emitters and a rectangular shaped beam creates this anisotropy in the form of local heat generation. This makes it possible to use AR-coated Cr:YAG crystal perpendicular to the laser beam instead of using a crystal in the Brewster angle which would have lengthened the cavity. Stable blue pulse parameters and efficient conversion to the blue indicate that the polarisation was close to linear.

With a short laser crystal and short cavity, the saturable absorber has to be located near the laser crystal on which the pump beam is focused. The intensity of the remaining part of the pump power is still high at the saturable absorber bleaching partially the Q-switch crystal and reducing the absorbance of the saturable absorber [6]. The above mentioned aspects create limitations and challenges that particularly concern a laser with the combination of high peak power and short pulse length.

3 SETUP

The general layout of the laser is depicted in Figure 1. The pump power was provided by a laser diode stack emitting at 808 nm. The output from the diode was collimated and focused onto the laser crystal with a pair of aspheric lenses with focal lengths of 13.8 mm and 18.4 mm. Figure 2 shows the pump spot at the focus where a round 80 μm-wide intensity maximum was surrounded by lower side maxima on the opposite sides of the center point. The length and transverse dimensions of the laser crystal were 1.5 mm and 5×5 mm^2, respectively.

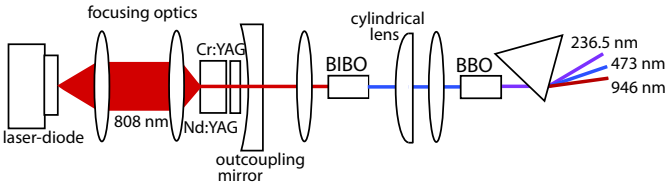

FIG. 1 Schematic picture of the setup. The blue beam is elongated by the walk-off in the BIBO crystal. Cylindrical lens collects the light in the fast diverging direction with smaller focus and sets the foci for both directions to the same position inside the $\beta-$BBO crystal.

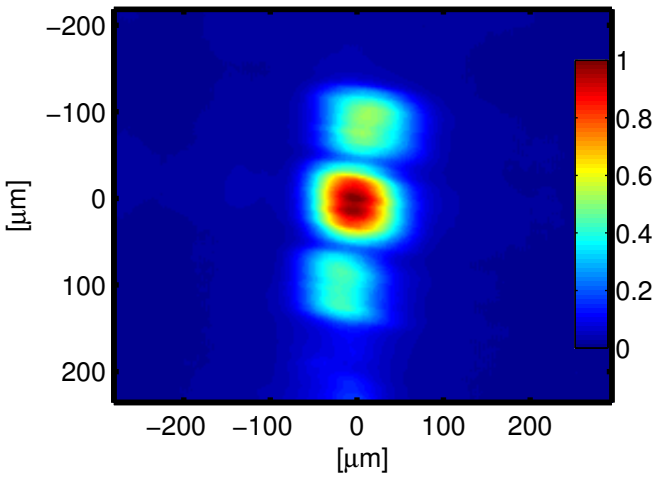

FIG. 2 Intensity distribution of the pump beam at the focus.

The rear surface of the crystal had a dielectric coating which is highly reflective at 946 nm and highly transmissive at 808 nm and 1064 nm. The laser cavity was formed between the coated rear surface of the crystal and the out-coupling mirror. The radius of curvature and reflectivity of the output coupler were 150 mm and 92%, respectively. A relatively large radius of curvature was chosen to give a large mode with the given cavity length. The cavity ends were highly transmissive at 1064 nm to prevent parasitic laser oscillation in this high-gain transition. The front surface of the laser crystal was anti-reflection (AR) coated at the laser wavelength.

The laser crystal was doped with 1% of Nd which leads to 47% absorption of the pump power in the 1.5 mm-long crystal. Efficient cooling of the active material was facilitated by circulating water with the temperature of 20°C through the crystal mount made of copper. Passive Q-switching was done by placing an AR coated Cr^{4+}:YAG crystal with unsaturated transmission of 96.5% to the cavity. The transverse dimensions of the crystal were 4×4 mm^2 and the thickness was 0.35 mm. The ground and exited state cross sections for Cr:YAG at 946 nm are 4.0×10^{-18} cm^2 and 1.1×10^{-18} cm^2, respectively [7]. Active ion concentration calculated from the transmission at the unsaturated absorption of the crystal was 2.5×10^{17} 1/cm^3. The free propagation length was minimized so that the physical length of the cavity was 3.5 mm.

A lens with the focal length of 5 cm was placed in a distance of 13.2 cm from the laser output coupling mirror. The conversion from 946 to 473 nm was performed in a 1 cm-long BIBO crystal. The walk-off angle of this process is 40.7 mrad and the phase matching angle $\theta = 161.7°$ and $\phi = 90°$ [8]. The intensity of the blue beam at the focus [9] in the BIBO crystal and the Gaussian fits to the corresponding cross sections are presented in Figure 3. The Gaussian fits gave FWHM beam

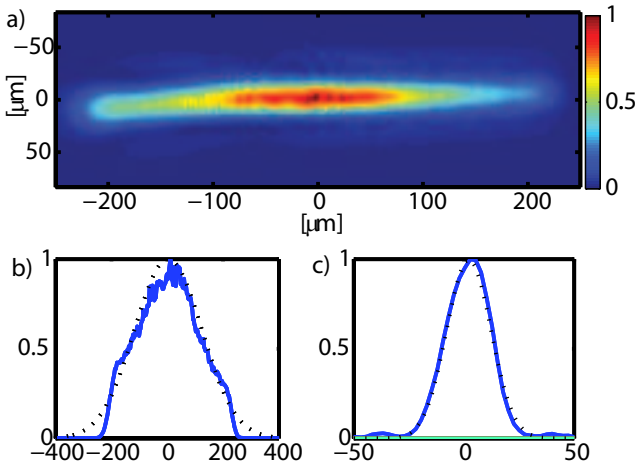

FIG. 3 a) Blue beam intensity at the focus in the BIBO crystal imaged to a beam camera. Measured cross sections (solid) and Gaussian fits (dotted) in the walk-off b) and perpendicular to walk-off c) directions. FWHM beam widths are 283 b) and 27 μm c).

widths of 280 μm and 27 μm in the walk-off and perpendicular to the walk-off directions, respectively. The elliptic beam diverged faster in the direction of the narrower cross section and it was collected with a cylindrical lens of a focal length of 30 mm. The position of the lens was 2.6 cm behind the BIBO crystal. This lens gave some freedom to modify foci for different cross sectional directions of the beam in the $\beta-$BBO crystal with phase matching angle $\theta = 57.5°$. The optimal conversion from blue to UV in $\beta-$BBO can be achieved with an elliptic beam with axes of 56 and 14 μm (FWHM) [8, 10]. The elliptic shape is due to the high walk-off conversion process with an angle of 80.5 mrad. After the cylindrical lens the blue beam was focused to the $\beta-$BBO crystal with a spherical lens having a focal length of 40 mm. It was placed in a distance of 14 cm from the BIBO crystal. The lens was AR coated for the visible light. The laser beams with variable wavelengths were finally separated with a prism that was transparent to UV. An aperture was used to reduce the pump power in the power measurements of 946, 473 and 236 nm. A long pass filter with the cut-off wavelength of 850 nm was used in power measurements for 946 nm. Bandpass filter BG40 was used to filter out 946 and 808 nm in the measurement of the blue beam. When measuring UV power, the scattered background light at other wavelengths was determined by tilting the BBO crystal in to such an angle that no phasematching occured. This background power value was reduced from the corresponding UV-power reading.

The birefringently phasematched nonlinear crystals of BBO, LBO and BIBO can be used for converting light from IR to blue. All of these processes are type I phasematched. The BIBO crystal was chosen because of the highest nonlinearity and moderate walk-off. LBO has the lowest walk-off but at the same time notably lower nonlinear coefficient than BIBO. The BBO has both lower nonlinearity and higher walk-off than BIBO crystal. The specifications of these three crystals are listed in Table 1.

nonlinear material	walk-off angle [mrad]	nonlinear coefficient [pm/V]
BIBO	40.7	3.3
BBO	60.3	2.0
LBO	11.3	0.8

TABLE 1 Specifications of birefringently phasematched nonlinear crystals for second harmonic generation of 946 nm [8].

4 RESULTS

A graph presenting the average power of the laser at 946 and 473 nm together with the repetition rate as a function of the absorbed pump power is presented in Figure 4. The following results were measured with the absorbed pump power of 3.3 W which was 45% of the incoming pump power. The average power at the wavelength of 946 nm was 388 mW. The M^2 values at 946 nm for the two transverse axes were measured to be 1.0 and 1.1, indicating that the beam is diffraction limited within the measurement accuracy.

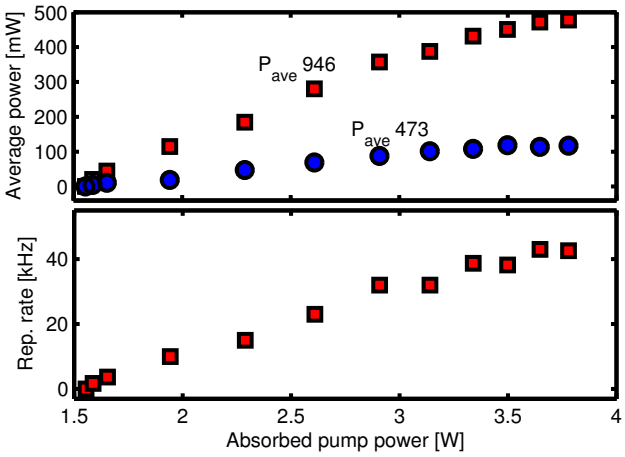

FIG. 4 Average laser power at 946 and 473 nm and the repetition rate as a function of the absorbed pump power.

Secondary pulses were observed frequently after the main laser pulse at the wavelength of 946 nm. This phenomenon is proposed to be related to a bottleneck effect during the laser pulse [11, 12]. Degnan *et al.* considers that the bottleneck would be formed because of the thermalization among the Stark sublevels whereas Ng *et al.* suggests that the delay would be caused by the finite lifetime of the lower laser level. The effect depends on the relaxation parameter which is a product of the relaxation rate and the photon lifetime in the resonator [11]. Optimising the alignment did not lead to the

disappearance of the satellite pulses. The portion of the laser energy in the satellite pulses was measured to be around 14%. A typical IR laser pulse with a satellite pulse is shown in Figure 5. The blue satellite pulse was barely observable, because of the poor conversion of weaker satellite pulse in comparison to the main pulse. The average power of the main pulses were 330 mW, pulse width was 3.5 ns, and repetition rate 35 kHz. The energy of the main pulse was 9.4 μJ and the peak power 2.7 kW. Standard deviations for short term pulse width and the period between the pulses were 2% and 12%, respectively.

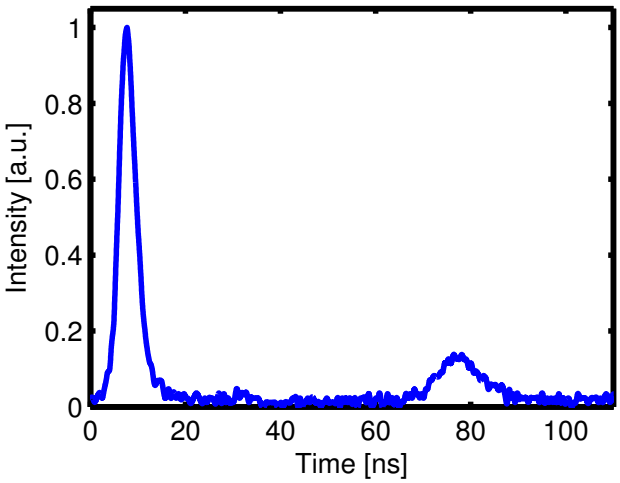

FIG. 5 A time trace of a single 946 nm laser pulse with a typical satellite pulse.

The pulse energy in the blue was 3.0 μJ resulting in conversion of 31% from the main pulse which is close to the simulated value of 29% [8]. The conversion from the measured average power with the satellite pulses was 28%. Pulse length at 473 nm was 2.4 ns and peak power 1.2 kW. The position of the focusing lens for conversion to the blue was determined so that the focus in the BIBO was measured to be near the optimal focus of 28 μm (FWHM) [8]. The UV power was optimised by adjusting the positions of the cylindrical and spherical lenses. The best average UV power was obtained with a focus axes of 36 and 24 μm. With this kind of optical path, foci for vertical and horizontal directions were confirmed to be in the same position in the following measurements with the beam camera.

The intensity distribution of the blue beam was recorded with the beam camera from the focus to 24 mm with 3 mm steps and it is presented in Figure 6. The M^2 value calculated using the second moment method for perpendicular to the walk-off and the walk-off directions gave values of 1.4 and 2.1, while the theoretical values are 1.13 and 1.8, respectively [8].

We used a fast photo detector [13] with 100 ps rise time to measure the blue and IR pulse widths. For UV-pulse measurements we used a detector [14] with a 1 ns rise time because the wavelength of 236 nm was not in the spectral response range of the detector with faster response. The time constant for the detector used for UV measurements was obtained by comparing the time responses of the two detectors for the blue pulses. This obtained time constant was then used to calculate

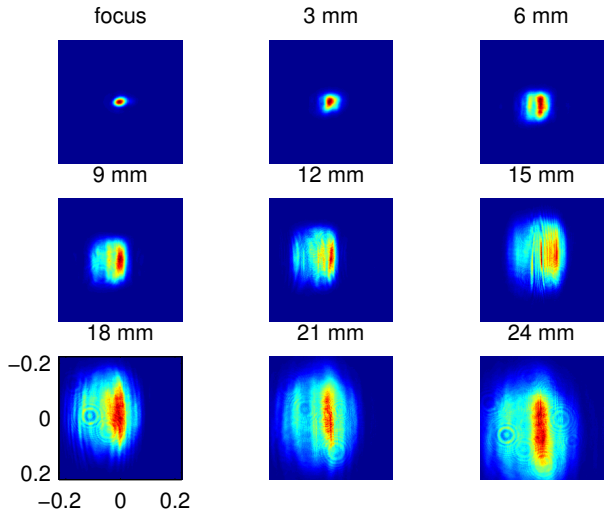

FIG. 6 Intensity [a.u.] of the blue laser beam at the focus at the place of the $\beta-$BBO crystal and after the focus with the steps of 3 mm. Axial measures are in millimeters.

an estimate of 1.9 ns for the UV pulse length. Average power at 236 nm was 7.6 mW the pulse energy of 230 nJ, and peak power of 120 W.

The conversion efficiencies were simulated for diffraction limited beams with different beam sizes and using the measured pulse parameters. The simulated maximum conversion with an optimal elliptic beam is 15%. The conversion is 12% for the beam size that was used in the experiments and 11% for the best spherical beam with 23 μm beam width [8]. The experimental conversion from blue to UV was 7%. This is in good agreement with the simulations since some reduction of the conversion efficiency is expected due to the somewhat degraded beam after the second harmonic generation from IR to blue.

5 CONCLUSIONS

A compact UV-laser source producing short pulses at 236 nm was constructed. A passively Q-switched quasi-three-level Nd:YAG laser at 946 nm was frequency doubled into blue with a conversion efficiency of 28% and to UV from blue with a conversion efficiency of 7% with BIBO and $\beta-$BBO nonlinear crystals, respectively. Average power at 236 nm was 7.6 mW with the pulse length of 1.9 ns, energy of 230 nJ, and peak power of 120 W.

ACKNOWLEDGMENTS

This work was supported by the Graduate School of Electrical and Communications Engineering, the Finnish Foundation of Technology and Finnish Academy of Science and Letters.

References

[1] Photon Systems, http://www.photonsystems.com/

[2] S. Chadha, R. Manoharan, P. Moënne-Loccoz, W. H. Nelson, W. L. Peticolas, and J. F. Sperry, "Comparison of the UV resonance

Raman spectra of bacteria, bacterial cell walls, and ribosomes excited in the deep UV" Appl. Spectrosc. **47**, 38–43 (1993).

[3] O. Kimmelma, M. Kaivola, I. Tittonen, and S. C. Buchter,"Short pulse, high peak power, diode pumped, passively Q-switched 946 nm Nd:YAG laser" Opt. Commun. **273**, 496–499 (2007).

[4] S. Johansson, S. Bjurshagen, C. Canalias, V. Pasiskevicius, F. Laurell, and R. Koch, "An all solid-state UV source based on a frequency quadrupled, passively Q-switched 946 nm laser" Opt. Express **15**, 449–458 (2007).

[5] D. C. Gerstenberger, T. M. Trautmann, and M. S. Bowers, "Noncritically phase-matched second-harmonic generation in cesium lithium borate" Opt. Lett. **28**, 1242–1244 (2003).

[6] J. Zayhowski, and A. Wilson, Jr, "Pump-Induced Bleaching of the Saturable Absorber in Short-Pulse Nd:YAG/Cr^{4+}:YAG Passively Q-Switched Microchip Lasers" IEEE J. Quantum Elect. **39**, 1588–1593 (2003).

[7] X. Zhang, A. Brenier, J. Wang, and H. Zhang, "Absorption cross-section of Cr^{4+}:YAG at 946 and 914 nm" Opt. Mater. **26**, 293–296 (2004).

[8] SNLO version 41 nonlinear optics code available from A. V. Smith, Sandia National Laboratories, Albuquerque, NM 87185-1423.

[9] The blue beam focus in the BIBO crystal was imaged to a beam camera with a 40 mm focal length lens. The used beam camera was Ophir Beamstar-Fx-50 with a 4-times beam expander.

[10] T. Freegarde, J. Coutts, J. Walz, D. Leibfried, and T.W. Hänsch, "General analysis of type I second-harmonic generation with elliptical Gaussian beams" J. Opt. Soc. Am. B-Opt. **14**, 2010–2016 (1997).

[11] J. J. Degnan"Effects of thermalization on Q-switched laser properties" IEEE J. Quantum. Elect. **34**, 887–899 (1998).

[12] S.P. Ng, D. Y. Tang, L. J. Qian, and L. J. Qin, "Satellite Pulse Generation in Diode-Pumped Passively Q-Switched Nd:GdVO4 Lasers" IEEE J. Quantum. Elect. **42**, 625–632 (2006).

[13] Newport D-100 photo detector

[14] Thorlabs DET210 photo detector